Available online at www.sciencedirect.com
SCIENCE DIRECT®
Phytochemistry 65 (2004) 323–330
PHYTOCHEMISTRY
www.elsevier.com/locate/phytochem

Carbon and hydrogen isotopic fractionation during lipid biosynthesis in a higher plant (*Cryptomeria japonica*)

Yoshito Chikaraishi[a,*], Hiroshi Naraoka[a], Simon R. Poulson[b]

[a]*Department of Chemistry, Tokyo Metropolitan University, 1-1, Minami-Ohsawa, Hachioji, Tokyo 192-0397, Japan*
[b]*Department of Geological Science, MS-172, University of Nevada-Reno. Reno, Nevada 89557-0138, USA*

Received in revised form 13 November 2003

Abstract

Compound-specific carbon and hydrogen isotopic compositions of lipid biomolecules (*n*-alkanes, *n*-alkanoic acids, *n*-alkanols, sesquiterpenes, diterpenes, phytol, diterpenols and β-sitosterol), extracted from *Cryptomeria japonica* leaves, were determined in order to understand isotopic fractionations occurring during lipid biosynthesis in this species. All lipid biomolecules were depleted in both ^{13}C and D relative to bulk tissue and ambient water, respectively. *n*-Alkyl lipids associated with the acetogenic pathway were depleted in ^{13}C relative to bulk tissue by 2.4–9.9‰ and depleted in D relative to ambient water by 91–152‰. C_{15}- and C_{30}-isoprenoid lipids (sesquiterpenes, squalene and β-sitosterol) associated with the mevalonic-acid pathway are depleted in ^{13}C relative to bulk tissue by 1.7–3.1‰ and depleted in D relative to ambient water by 212–238‰. C_{20}-isoprenoid lipids (phytol and diterpenoids) associated with the non-mevalonic-acid pathway were depleted in ^{13}C relative to bulk tissue by 4.6–5.9‰ and depleted in D relative to ambient water by 238–303‰. Phytol was significantly depleted in D by amounts up to 65‰ relative to other C_{20} isoprenoid lipids. The acetogenic, mevalonic-acid and non-mevalonic-acid pathways were clearly discriminated using a cross-plot between the carbon and hydrogen isotopic fractionations.

Keywords: *Cryptomeria japonica*; Taxodiaceae; δD; $\delta^{13}C$; Isotopic fractionation; Lipid biosynthesis; Acetogenic; Mevalonic-acid; Methylerythritol-phosphate

1. Introduction

Knowledge of isotopic compositions and fractionation of individual lipid biomolecules in primary producers such as terrestrial and aquatic plants is biologically and geochemically significant (e.g. Hayes, 2001). Isotopic compositions of lipid biomolecules should be closely related to isotopic fractionation during photosynthesis and lipid biosynthesis. Carbon isotopic fractionation during photosynthesis has been well studied (e.g. Deines, 1980), with different mechanisms and fractionations among the different types of carbon fixation (such as C3, C4 and CAM plants). On the other hand, hydrogen isotopic fractionation during photosynthesis has not been studied extensively. Hydrogen in leaf water is utilized when nicotinamide adenine dinucleotide phosphate ($NADP^+$) is reduced to form NADPH. NADPH then reacts with 3-phosphoglyceric acid (3-PGA) (**1**) to form glyceraldehyde-3-phosphate (GA-3-P) (**2**) in the Calvin-Benson cycle (photosynthetic reductive pentosephosphate cycle) (see Fig. 1 for structures). Yakir and DeNiro (1990) reported that the net isotope effect associated with photosynthesis was estimated to be −171‰ because large isotopic fractionations occurred during NADPH formation. In lipid biosynthesis, carbon and hydrogen isotopic fractionations also occur during various biochemical reactions such as decarboxylation of pyruvate (**3**) to form acetate (**4**) (DeNiro and Epstein, 1977; Monson and Hayes, 1982) and hydrogenation with NADPH (Smith and Epstein, 1970; Luo et al., 1991), respectively. Generally, lipid biomolecules are biosynthesized from isotopically light acetate (**4**) precursors, and additional isotopic fractionations occur at branch points in the biosynthetic pathways (Hayes, 1993). As a result, lipid biomolecules have various isotopic compositions depending upon their biosynthetic origins. In higher plants, typical lipid

* Corresponding author. Fax: +81-426-77-2525.
E-mail address: rikie@comp.metro-u.ac.jp (Y. Chikaraishi).

0031-9422/$ - see front matter © 2003 Elsevier Ltd. All rights reserved.
doi:10.1016/j.phytochem.2003.12.003

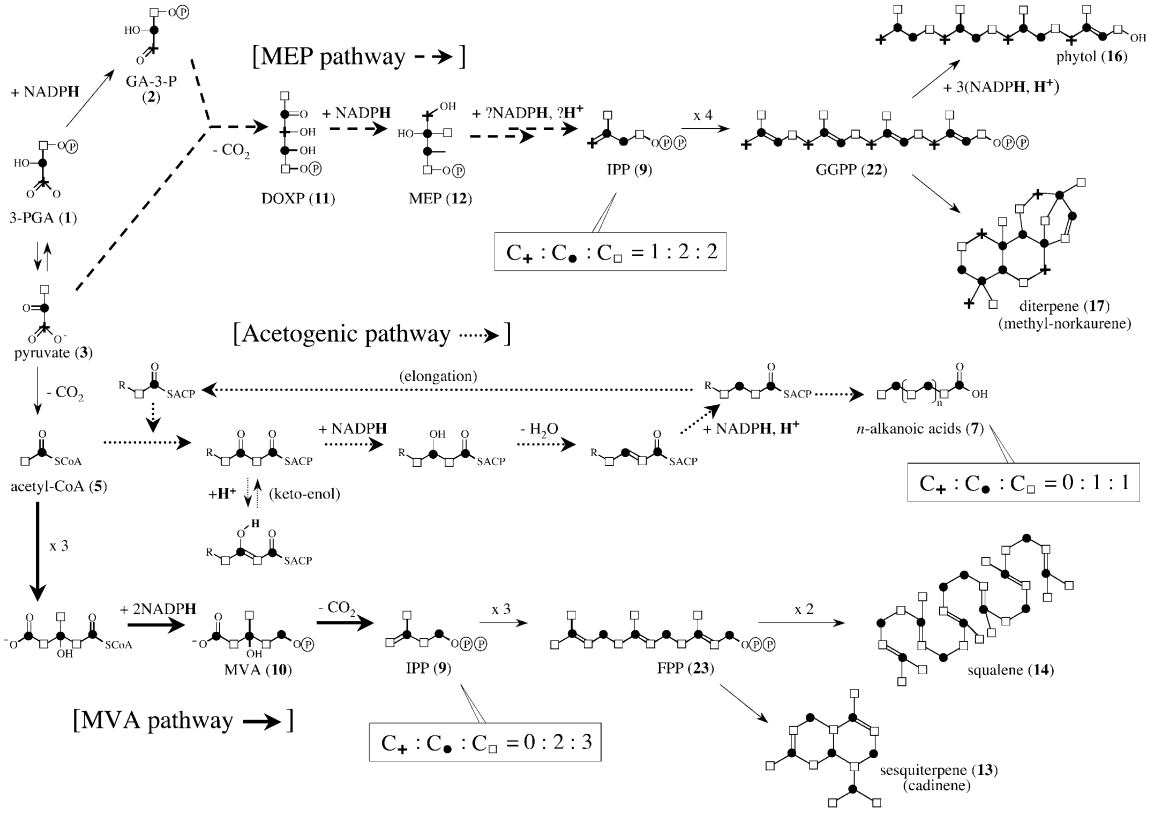

Fig. 1. The relationships between carbon and hydrogen sources with respect to positions in the typical lipid biomolecules associated with acetogenic, MVA (**10**) and MEP (**12**) pathways (after Cvejic and Rohmer 2000; Lange et al., 2000; Eisenreich et al., 2001; Hayes 2001; Sessions et al., 2002). Carbon atoms derived from C-1, C-2 and C-3 positions of 3-PGA (**1**) are drawn by crosses, filled circles and open squares, respectively. Lipid biomolecules have different ratio of carbon sources among the acetogenic, MVA (**10**) and MEP (**12**) pathways. Hydrogen of NADP**H** and **H**$^+$ in cell water are used in various reduction or exchange reactions. Abbreviations: NADP$^+$: nicotinamide adenine dinucleotide phosphate; 3-PGA: 3-phosphoglyceric acid (**1**); GA-3-P: D-glyceraldehyde-3-phosphate (**2**); acetyl–CoA: acetyl coenzyme-A (**5**); IPP: isopentenyl pyrophosphate (**9**); MVA: mevalonic acid (**10**); DOXP: 1-deoxy-D-xylulose-5-phosphate (**11**); MEP: 2-C-methyl-D-erythritol-4-phosphate (**12**); GGPP: geranylgeranyl pyrophospate (**22**); FPP: farnesyl pyrophosphate (**23**).

biomolecules are related to three different biosynthetic pathways. The straight-chain molecules, termed *n*-alkyl lipids, are biosynthesized in the acetogenic pathway with an acetyl coenzyme-A (acetyl–CoA) (**5**) biosynthetic precursor. They include *n*-alkanes (**6**), *n*-alkanoic acids (**7**) and *n*-alkanols (**8**). *n*-Alkanes (**6**) and *n*-alkanols (**8**) are biosynthesized from *n*-alkanoic acids (**7**) by enzymatic decarboxylation and reduction, respectively (Eglinton and Hamilton, 1967; Kolattukudy, 1976). In contrast, all isoprenoid lipids are constructed from isopentenyl pyrophoshate (IPP) (**9**). IPP (**9**) is produced by two pathways in higher plants: the mevalonic-acid (MVA) (**10**) pathway or non-mevalonic-acid pathway, which is termed the 1-deoxy-D-xylulose-5-phosphate (DOXP) (**11**) or 2-C-methyl-D-erythritol-4-phosphate (MEP) (**12**) pathway (e.g. Kleinig, 1989). One IPP (**9**) is biosynthesized by the MVA (**10**) pathway within the cytosol to form C_{15}- and C_{30}-isoprenoid lipids such as sesquiterpenes (**13**), squalene (**14**) and sterols (e.g. **15**), while another IPP (**9**) is biosynthesized by the MEP (**12**) pathway within the chloroplast to form C_{20}-isoprenoid lipids such as phytol (**16**) and diterpenoids (**17–21**) (e.g. Arigoni et al., 1997; Lichtenthaler et al., 1997; Bohlmann et al., 1999; Lichtenthaler, 1999). Carbon and hydrogen isotopic fractionations during lipid biosyntheses have been reported in previous studies (e.g. for carbon: Monson and Hayes, 1982; and for hydrogen: Sessions et al., 1999). For example, Monson and Hayes (1982) reported a ^{13}C-depletion mechanism for *n*-alkanoic acids (**7**) in the acetogenic pathway, whereas Sessions et al. (1999) reported that phytol (**16**) was depleted in D relative to sterols (e.g. **15**) by 50‰. The latter proposed that this difference could be due to isotopically distinct pools of NADPH in the cytosol and chloroplast, because sterols (e.g. **15**) and phytol (**16**) are biosynthesized within the cytosol and chloroplast, respectively. Although carbon and hydrogen isotopic fractionations of lipid biomolecules can provide useful information on their biosyntheses associated with the various pathways, the detailed dual (δ^{13}C-δD) isotopic signatures have been poorly characterized.

The purpose of this study was to investigate compound-specific carbon and hydrogen isotopic compositions of typical lipid biomolecules [*n*-alkanes (**6**),

n-alkanoic acids (**7**), *n*-alkanols (**8**), sesquiterpenes (**13**), squalene (**14**), β-sitosterol (**15**), phytol (**16**), diterpenes (**17**) and diterpenols (**18–21**)] extracted from *Cryptomeria japonica* (see Fig. 2). Furthermore, this study will quantify carbon and hydrogen isotopic fractionations associated with various lipid biosynthetic pathways. *Cryptomeria japonica* is a representative C3-gymnosperm cedar, being widely distributed throughout Japan, as well as globally.

2. Results and discussion

2.1. Molecular distributions

n-Alkanes (C_{25}–C_{35}) (**6**), sesquiterpenes (several isomers of cadinene) (**13**) and diterpenes (several isomers of methyl-norkaurene) (**17**) were identified in the hydrocarbon fraction, whereas *n*-alkanoic acids (C_{12}–C_{36}) (**7**) and *n*-alkanols (C_{22}–*n*-C_{32}) (**8**) were found in the *n*-alkanoic acid (**7**) and *n*-alkanol (**8**) fractions, respectively. Squalene (**14**), 24-ethylcholest-5-en-3β-ol (β-sitosterol) (**15**), phytol (**16**) and diterpenols [such as sandaracopimarinol (**18**) ferruginol (**19**) and sugiol (**21**)] were present in the isoprenoid alcohol fraction. These lipid biomolecules are typically found in higher plants [e.g. *n*-alkyl lipids (**6–8**): Eglinton and Hamilton (1967); β-sitosterol (**15**): Killops and Killops (1993); phytol (**16**): Collister et al. (1994); and ferruginol (**19**): Chang et al. (2001)]. No significant difference was found in the molecular distributions (e.g. concentration and carbon number) between spring and autumn samples (Table 1).

2.2. Compound-specific carbon and hydrogen isotopic compositions

Carbon and hydrogen isotopic compositions of individual lipid biomolecules are summarized in Table 1. By comparison, isotopic compositions of sesquiterpenes (**13**) and diterpenes (**17**) are reported as combined values with the same carbon-numbered isomers, because these could not be resolved for isotope analysis in this study. *n*-Alkyl lipids [*n*-alkanes (**6**), *n*-alkanoic acids (**7**) and *n*-alkanols (**8**)] have $\delta^{13}C$ values of −29.5‰ to −36.9‰ and δD values of −129‰ to −188‰. C_{15}- and C_{30}-isoprenoid lipids [sesquiterpenes (**13**), squalene (**14**) and β-sitosterol (**15**)] have $\delta^{13}C$ values of −28.0‰ to −31.0‰ and δD values of −245‰ to −270‰. C_{20}-isoprenoid lipids [phytol (**16**) and diterpenids (**17–21**)] have $\delta^{13}C$ values of −31.1‰ to −33.4‰ and δD values of −270‰ to −332‰. In C_{20}-isoprenoid lipids, phytol (**16**) is significantly depleted in D (δD values of −326‰ to −332‰) relative to other C_{20} isoprenoid lipids (**17–21**). Generally, lipid biomolecules in spring leaf tissues were are enriched in both ^{13}C (1.4‰ on average) and D (5‰ on average) relative to autumn leaves, in which this isotopic relationship were also seen in $\delta^{13}C$ value of bulk tissue and δD value of cellulose nitrate (Table 1). Although this may indicate slight differences in growth-rate and water-efficiency in different seasons (e.g. Lockheart et al., 1997), isotopic compositions of spring and autumn leaves showed no significant signature in this study. The $\delta^{13}C$ and δD values of several lipid biomolecules measured in this study were thus similar to other values available in the literature [e.g. $\delta^{13}C$ for *n*-alkanes (**6**): Collister et al. (1994); Lockheart et al. (1997, 1998); Reddy et al. (2000), $\delta^{13}C$ for *n*-alkanoic acids (**7**): Ballentine et al. (1998), $\delta^{13}C$ values for β-sitosterol (**15**): Lockheart et al. (1997), $\delta^{13}C$ for phytol (**16**): Collister et al. (1994), δD for *n*-alkyl lipids (**6–8**), β-sitosterol (**15**) and phytol (**16**): Sessions et al. (1999)].

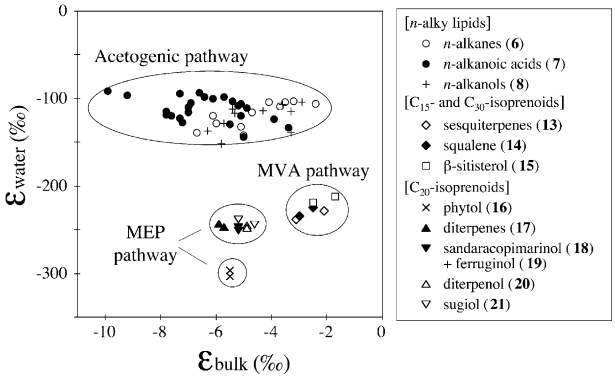

Fig. 2. The ϵ_{bulk}–ϵ_{water} of observed lipid biomolecules in *Cryptomeria japonica*.

2.3. Isotopic fractionations

The carbon isotopic fractionation between a lipid biomolecule and bulk tissue (ϵ_{bulk}) is defined in Eq. (1). Similarly, the hydrogen isotopic fractionation between a lipid biomolecule and ambient water (ϵ_{water}) is defined in Eq. (2).

$$\varepsilon_{bulk} = 1000\left[\left(\delta^{13}C_{lipid} + 1000\right)/\left(\delta^{13}C_{bulk} + 1000\right) - 1\right] \quad (1)$$

$$\varepsilon_{water} = 1000\left[\left(\delta D_{lipid} + 1000\right)/\left(\delta D_{water} + 1000\right) - 1\right] \quad (2)$$

$\delta^{13}C$ values of bulk tissues ($\delta^{13}C_{bulk}$) and δD values of ambient water (δD_{water}) have been measured previously (Chikaraishi and Naraoka, 2003), with a δD_{water} value of −42‰ as an annual mean value of precipitation (ranging from −74 to −10‰). Calculated ϵ_{bulk} and ϵ_{water} values of isolated lipid biomolecules are shown in Fig. 1. All lipid biomolecules were depleted in both ^{13}C and D relative to bulk tissue and ambient water, respectively. *n*-Alkyl lipids (**6–8**) associated with the acetogenic pathway had wide variations in both ϵ_{bulk} (−2.4‰ to −9.9‰) and ϵ_{water} (−91‰ to −152‰) values, whereas

C_{15}- and C_{30}-isoprenoid lipids (**13**–**15**) associated with the MVA (**10**) pathway had a relatively narrow range of both ϵ_{bulk} (−1.7‰ to −3.1‰) and ϵ_{water} (−212‰ to −238‰) values. C_{20}-isoprenoid lipids (**16**–**21**) associated with the MEP (**12**) pathway had ϵbulk values of −4.6‰ to −5.9‰ and ϵ_{water} values of −238‰ to −303‰, but phytol (**16**) was significantly depleted in D (ϵ_{water} values of −296‰ to −303‰) by up to 65‰ relative to other C_{20} isoprenoid lipids (**17**–**21**). Thus, lipid biomolecules from the acetogenic, MVA (**10**) and MEP (**12**) pathways were clearly discriminated using the ϵ_{bulk}–ϵ_{water} cross plot (Fig. 1).

In the case of carbon, biosynthetically equivalent lipid biomolecules [such as sesquiterpenes (**13**), squalene (**14**) and β-sitosterol (**15**)] had similar ϵ_{bulk} values. Moreover, the ϵ_{bulk} values associated with the MVA (**10**) pathway were clearly distinct from those associated with the MEP (**12**) pathway. Although the specific mechanisms responsible for these differences are not yet been known, two possibilities can be considered: (1) lipid biomolecules are derived from isotopically distinct precursors in each of the three pathways, and/or 2) the kinetic isotope effects associated with specific reactions may differ in each biosynthetic pathway. As shown in Fig. 2, lipid

Table 1
Compound-specific $\delta^{13}C$ and δD values of lipid biomolecules extracted from *Cryptomeria japonica*

	Spring					Autumn				
Compounds	μg/g dry	$\delta^{13}C$ (‰)	S.D. (‰)	δD (‰)	S.D. (‰)	μg/g dry	$\delta^{13}C$ (‰)	S.D. (‰)	δD (‰)	S.D. (‰)
Bulk tissue[a]		−26.4	0.4				−27.9	0.03		
Cellulose (**24**) nitrate				−101	2				−106	5
n-Alkane[a] (**6**)										
25	1			−169	5	1	−34.4	0.2	−175	4
27	6	−32.2	0.2	−165	0	7	−32.7	0.3	−178	3
29	3	−32.3	0.2	−156	6	2	−32.9	0.3	−168	1
31	5	−30.4	0.3	−141	5	3	−32.5	0.5	−153	1
33	72	−29.5	0.4	−140	5	65	−31.5	0.1	−146	1
35	20	−29.8	0.4	−141	2	18	−30.3	0.4	−144	10
n-Alkanoic acid (**7**)										
12	82	−30.2	0.0	−159	5	42	−31.2	0.2	−169	2
14	263	−33.8	0.1	−157	5	134	−34.9	0.3	−163	3
16	1941	−36.1	0.2	−129	7	1141	−36.9	0.2	−134	4
18	106	−32.8	0.3	−131	3	55	−34.1	0.2	−136	2
20	61	−31.4	0.1	−145	0	35	−32.8	0.5	−157	3
22	103	−31.7	0.2	−165	3	50	−32.7	0.2	−180	1
24	48	−31.4	0.1	−144	5	24	−32.7	0.2	−148	4
26	16	−32.3	0.3	−138	4	8	−34.6	0.3	−143	5
28	68	−34.0	0.2	−153	4	35	−35.5	0.2	−156	2
30	26	−33.2	0.4	−153	3	13	−35.0	0.2	−159	3
32	25	−33.5	0.1	−133	4	15	−34.7	0.4	−147	1
34	29	−31.9	0.0	−136	4	18	−33.2	0.2	−141	3
n-Alkanol (**8**)										
22	10	−29.6	0.3	−175	2	8	−30.7	0.2	−141	4
24	13	−29.6	0.2	−152	5	9	−31.4	0.2	−145	2
26	29	−30.6	0.1	−151	3	21	−33.4	0.3	−164	1
28	39	−32.6	0.1	−173	4	29	−33.6	0.0	−188	4
30	8	−31.7	0.2	−167	5	7	−33.0	0.1	−155	5
32	10	−31.6	0.1	−144	3	7	−33.2	0.3	−150	3
Isoprenoid										
sesquiterpenes[b] ($C_{15}H_{24}$) (**13**)	671	−28.5	0.1	−260	2	165	−31.0	0.4	−270	2
squalene (**14**)	56	−28.8	0.3	−258	3	39	−30.8	0.2	−266	4
b−sitosterol (**15**)	463	−28.0	0.5	−245	6	371	−30.3	0.3	−252	4
phytol (**16**)	861	−31.7	0.5	−326	5	621	−33.2	0.3	−332	5
diterpenes[b] ($C_{20}H_{32}$) (**17**)	1532	−32.1	0.2	−275	5	910	−33.4	0.2	−279	3
sandaracopimarinol (**18**)	1454	−31.4	0.4	−279	6	1141	−33.0	0.3	−282	4
+ferruginol[c](**19**)										
diterpenol ($C_{20}H_{32}O$)[d] (**20**)	1065	−31.1	0.2	−277	4	746	−32.7	0.4	−280	3
sugiol[e] (**21**)	43	−31.5	0.4	−270	3	37	−32.4	0.3	−276	4

[a] Reported in Chikaraishi and Naraoka (2003).
[b] Combined values with the same carbon number isomers (specific identification could not be determined).
[c] Combined values sandaracopimarinol (**18**) and ferruginol (**19**).
[d] Specific identification could not be determined.
[e] Combined values of sugiol (**21**) with before and after coeluting diterpenol peaks (specific identification could not be determined).

biomolecules had different ratios of carbon sources among the acetogenic, MVA (**10**) and MEP (**12**) pathways. All carbons in lipid biomolecules associated with the acetogenic and MVA (**10**) pathways were derived from C-2 (filled circle in Fig. 2) and C-3 (open square) positions of 3-PGA (**1**), with different constituting carbon ratios (filled circle/open square). On the other hand, lipid biomolecules associated with the MEP (**12**) pathway contain several carbons derived from the C-1 (cross) positions of 3-PGA (**1**) (Fig. 2). In addition, kinetic isotope effects during various biochemical reactions (such as condensation and decarboxylation) related to branch points in the pathways could cause isotopically distinct precursors among the acetogenic, MVA (**10**) and MEP (**12**) pathways (e.g. Hayes, 1993; 2001). For example, an isotope effect during decarboxylation of pyruvate (**3**) to form acetyl–CoA (**5**) causes depletion in ^{13}C at the carbonyl carbon (filled circle in Fig. 2), and leaves the methyl carbon (open square) unfractionated. The ϵbulk values associated with the acetogenic pathway had wide variations (−2.4‰ to −9.9‰), and could not be discriminated from the MVA (**10**) (−1.7‰ to −3.1‰) and MEP (**12**) (−4.6‰ to −5.9‰) pathways. The large range of ϵ_{bulk} values for biomolecules produced by the acetogenic pathway may therefore be the result of many intermediate biomolecules in elongation having multiple fates [e.g. to form *n*-alkanes (**6**), *n*-alkanoic acids (**7**), *n*-alkanols (**8**) and their unsaturated derivatives, at various carbon numbers].

In the case of hydrogen, lipid biomolecules are biosynthesized by isotopically distinct hydrogen sources such as NADPH and cell water (H^+), as a result of various redox and exchange reactions (Fig. 1). Yakir and DeNiro (1990) reported that the first products of photosynthesis were depleted in D by 171‰ relative to cell water, and suggested that hydrogen from NADPH could be strongly depleted in D. The ϵ_{water} values of lipid biomolecules show a total range of −91‰ to −303‰ (Fig. 2). Particularly, *n*-alkyl lipids (**6–8**) are less depleted in D (ϵ_{water} values of −91‰ to −152‰) than isoprenoid lipids (**13–21**) (−212‰ to −303‰). This may be because keto −enol tautomerization in the acetogenic pathway increases the contribution of isotopically heavier cell water (perhaps, $\epsilon_{water} = 0$‰) into *n*-alkyl lipids (**6–8**) (Fig. 1). In keto −enol tautomerization, 75% of the hydrogen in *n*-alkyl lipids (**6–8**) is potentially subject to exchange with cell water (Sessions et al., 2002). On the other hand, phytol (**16**) was significantly depleted in D (ϵ_{water} values of −296‰ to −303‰) by up to 65‰ relative to diterpenoids (**17–21**), even though both phytol (**16**) and diterpenoids (**17–21**) are biosynthesized by a common IPP (**9**) precursor produced by the MEP (**12**) pathway within the chloroplast. Because the ϵ_{bulk} value of phytol (**16**) (∼−5.5‰) is very close to that of diterpenoids (**17–21**) (∼−5.2‰), no significant isotope effect of branch points at geranylgeranyl pyrophosphate (GGPP) (**22**) could be considered for carbon. Probably hydrogen isotopic fractionation is not expected at this branch point, either. Therefore, a significant D-depleted phytol (**16**) could be due to a kinetic isotope effect during hydrogenation to form phytol (**16**). Phytol (**16**) is biosynthesized by hydrogenation at three carbon double bonds of GGPP (**22**), using three NADPH and three H^+ of cell water. Assuming that the mean ϵ_{water} value of diterpenoids is similar to ϵ_{water} value for GGPP, the ϵ_{water} value of the six hydrogens added to phytol (**16**) is approximately −600‰. This suggests that a large kinetic isotope effect during the hydrogenation could be required from the GGPP (**22**) to phytol (**16**). A similar large hydrogen isotope effect (∼600‰) was reported during production of hydrogen gas by cyanobacteria (Luo et al., 1991). Thus, the ϵwater values of lipid biomolecules should depend on isotopically distinct hydrogen sources such as NADPH and/or H_2O, as well as an isotope effects invoked by redox or exchange reaction of hydrogen in lipid biosyntheses. Sessions et al. (1999) also suggested the existence of isotopically distinct pools of NADPH between the cytosol and chloroplast in order to explain the different ϵ_{water} values between sterols (e.g. **15**) and phytol (**16**). In this study, however, the ϵ_{water} values of sesquiterpenes (**13**) (−228‰ to −238‰) and squalene (**14**) (−225‰ to −251‰) are similar to those of diterpenoids (**17–21**) (−238‰ to −251‰), even though both sesquiterpenes (**13**) and squalene (**14**) were biosynthesized within the cytosol while diterpenoids (**17–21**) were biosynthesized within the chloroplast. Because the hydrogen sources during the reaction of MEP (**12**) to form IPP (**9**) in the MEP (**12**) pathway have not yet been identified, it is difficult to quantitatively compare the hydrogen sources among sesquiterpenes (**13**), squalene (**14**) and diterpenoids (**17–21**). The ϵwater values of isoprenoid lipids (**13–15**, **17–21**) in this study may suggest that NADPH within the cytosol and chloroplast are isotopically similar, and that extremely D-depleted phytol (**16**) is because of a large kinetic isotope effect during hydrogenation.

2.4. Concluding remarks

Compound-specific carbon and hydrogen isotopic compositions of lipid biomolecules [*n*-alkanes (**6**), *n*-alkanoic acids (**7**), *n*-alkanols (**8**), sesquiterpenes (**13**), squalene (**14**), β-sitosterol (**15**), phytol (**16**), diterpenes (**17**) and diterpenols (**18–21**)] have been determined in *C. japonica* leaves. In addition, carbon and hydrogen isotopic fractionations associated with various lipid biosynthetic pathways were quantified. The acetogenic, MVA (**10**) and MEP (**12**) pathways were clearly discriminated using a ϵ_{bulk}–ϵ_{water} cross plot (Fig. 2). These results suggest that the isotopic cross-plot ($\delta^{13}C$–δD or ϵ_{bulk}–ϵ_{water}) could be used as a quick means to assess

isoprenoid biosynthetic pathway present in prokaryotes, which is presently determined by fairly difficult genomic analysis. The ϵ_{bulk} values of lipid biomolecules depend on the acetogenic, MVA (**10**) and MEP (**12**) pathways, and the ϵ_{water} values depend on isotopically distinct hydrogen sources and/or isotope effects during reactions that involve hydrogen (such as redox and exchange reactions) in the lipid biosyntheses. In particular, a large hydrogen isotope effect during hydrogenation is proposed in order to produce the ϵwater values of individual lipid biomolecules. For example, the ϵwater value of six hydrogens added to form phytol (**16**) from GGPP (**22**) is estimated to be approximately −600‰. The ϵwater values of isoprenoid lipids (**13–21**) in this study may indicate no significant difference in δD values of NADPH and cell water between the cytosol and chloroplast.

3. Experimental

3.1. Samples

Fresh leaves of a *Cryptomeria japonica* plant from a forest in Gunma Prefecture (around lake Haruna), Japan were sampled in spring and autumn 1999 (Chikaraishi and Naraoka, 2003). Surface of leaves were cleaned with distilled water to remove contaminants, and were stored at −20 °C until analysis. Leaves were freeze-dried and crushed to a fine powder before analysis.

3.2. Preparation and δD analysis of cellulose nitrate (carbon-bound hydrogen in cellulose)

Cellulose (**24**) nitrate was prepared according to DeNiro (1981). In brief, powdered leaves were defatted by sonication with hexane and acetone extraction until the residues became colorless. The residues were delignified by sodium chlorite oxidation, and were then nitrated using a mixture of nitric acid and phosphorous-pentoxide (Epstein et al., 1976). Cellulose (**24**) nitrate was extracted from nitration products by dissolution in acetone, and precipitated from the acetone solution by adding distilled water. Prepared cellulose (**24**) nitrates were freeze-dried. Hydrogen isotopic analysis was carried out by elemental analyzer/isotope ratio mass spectrometer (EA/IRMS) using a Micromass IsoPrime interfaced with an Eurovector EA. The pyrolysis was performed with glassy carbon at 1290 °C. δD values are given in per mil (‰) relative to SMOW. Standard deviations of δD measurements were better than 4‰ (~1‰ in average). Isotopic precision was tested using NIST reference material 8540 (Polyethylene Foil 1, PEF1), and gave accurate values within the analytical standard deviations.

3.3. Lipid biomolecule preparations

Powdered leaves were saponified with 0.5 M Kou in MeOH:H_2O (95:5, w/w) by refluxing for 4.5 h and extracted by sonication with (Cu_2Ce_2/MeOH 2/1, v/v). The combined solutions (Kou/MeOH + Ca_2Ce_2/MeOH), were extracted with hexane/diethylether (9:1) to partition out neutral lipids. After addition of 12 N Hcl, the acidified solutions were extracted with hexane/diethylether (9:1) to obtain the acidic lipids. Neutral lipids were further separated into three fractions by silica gel cc. Hydrocarbons were eluted with hexane (100%) in the first fraction (N1 fraction); mono-alcohols and squalene (**14**) were eluted in the 2nd fraction (N2) with hexane/ethyl acetate (4:1). Fraction N2 was acetylated using acetic anhydride/pyridine (1:1 by volume, 1ml) and heating at 75 °C for 8 h. Acetylated N2 fractions were separated into straight-chain compounds (alkanol-acetate) and isoprenoid lipids (**14**–**16**, **18**–**21**) by forming urea adducts. The straight-chain compounds were separated into *n*-alkanol-acetates (**8**) and unsaturated alkanol-acetates by using $AsNO_3$ (10 wt.%) impregnated silica gel cc. *n*-Alkanol-acetates (**8**) were eluted with hexane/Cu_2Ce_2 (1:2); unsaturated alkanol-acetates were subsequently eluted with MeOH. Acidic lipids were esterified using 14% trifluorobromide/NeOH (100 °C for 1 h) to form fatty acid methyl esters (FAMEs). Methylesterified acidic lipids were separated into two fractions by silica gel cc. Mono-FAMEs were eluted with hexane/Cu_2Ce_2 (1:2) in the first fraction (A1 fraction). The mono-FAMEs were separated into saturated and unsaturated FAMEs using a silica gel cc impregnated with 10% (w/w) $AsNO_3$. Saturated FAMEs were eluted with hexane/ Cu_2Ce_2 (1:2); unsaturated FAMEs were subsequently eluted with hexane/EtOAc (1:1). Saturated FAMEs were separated into *n*-FAMEs [*n*-alkanoic acids (**7**)] and other FAMEs by forming urea adducts.

3.4. Identification and quantification

Lipid biomolecules were identified by GC/MS using a Hewlett Packard (HP) 6890 gas chromatograph connected to a HP MSD 5972 mass spectrometer. Individual compound concentrations were quantified using a HP 6890 GC with a flame-ionization detector, compared to the peak area of external *n*-alkane (**6**) standards.

3.5. Compound-specific δD and $\delta^{13}C$ analysis

Compound-specific carbon and hydrogen isotope analyses were carried out by GC/combustion/isotope ratio mass spectrometry (GC/combustion/IRMS) using a Finnigan Delta S interfaced with an HP5890GC and by GC/pyrolysis/IRMS using a Finnigan Delta plus XL interfaced with an HP6890GC, respectively. Combustion

was performed in a microvolume ceramic tube with CuO and Pt wires at 840 °C (Hayes, 1989). Pyrolysis was performed in a microvolume ceramic tube with graphite at 1440 °C (Hilkert et al., 1999). $\delta^{13}C$ and δD values are given in per mil (‰) relative to Peedee Belemnite (PDB) and Standard Mean Ocean Water (SMOW), respectively. Carbon and hydrogen isotopic compositions were calibrated by coinjected internal *n*-alkane (**6**) standards. δD values of standard *n*-alkanes (**6**) were determined relative to δD values of calibrated standards [*n*-alkanoic acids (**7**), *n*-alkanols (**8**), squalene (**14**), sterols (e.g. **15**) and phytol (**16**)] on GC/pyrolysis/IRMS analysis. Standard deviations of hydrogen and carbon isotope measurements were generally better than 7‰ (~3‰ in average) and 0.5‰ (~0.3‰ in average), respectively.

3.6. Correction of δD and $\delta^{13}C$ values for derivatized compounds

For *n*-alkanoic acids (**7**) and alcohols (**8**, **15**, **16**, **18**–**21**), $\delta^{13}C$ values of carbon in the underivatized compounds and the δD values of carbon-bound hydrogen are required. In the case of methyl esterification for *n*-alkanoic acids (**7**), the measured $\delta^{13}C$ and δD values of derivatized compounds were corrected by mass balance for the contribution of carbon ($\delta^{13}C$ values of −72.5‰) and hydrogen (δD values of −235‰) added during methyl esterification, because no isotopic fractionation was observed during methyl esterification (as determined by experiments with compounds of known isotopic compositions). In the case of acetylation of alcohols (**8**, **15**, **16**, **18**–**21**), the measured δD values of derivatized compounds were also corrected by mass balance for the contribution of hydrogen ($\delta D = -204$‰) added during acetylation, because no hydrogen isotopic fractionation was observed during acetylation. However, it is known that carbon isotopic fractionation occurs on carboxy-carbon during acetylation (Rieley, 1994). In this study, carbon isotopic composition of derivative carbon added during acetylation is calculated using two internal standards [*n*-hexadecanol (**25**) and *n*-octadecanol (**26**)] in the *n*-alkanol (**8**) fraction. The measured $\delta^{13}C$ values of derivatized compounds were corrected by isotopic mass balance.

Uncited reference

Hayes et al., 1989

Acknowledgements

We thank Mr. Naito for the assistance in the field. This work was supported by a Research Fellowship of the Japan Society for the Promotion of Science for Young Scientists (Y.C.) and a Grant-in-Aid for Scientific Research from the Japanese Ministry of Education, Science, Culture and Technology (H.N.).

References

Arigoni, D., Sagner, S., Latzel, C., Eisenreich, W., Bacher, A., 1997. Terpenoid biosynthesis from 1-deoxy-D-xylulose in higher plants by intramolecular skeletal rearrangement. Proceedings of the National Academy of Sciences of the United States of America 94, 10600–10605.

Ballentine, D.C., Macko, S.A., Turekian, V.C., 1998. Variability of stable carbon isotopic compositions in individual fatty acids from combustion of C4 and C3 plants: implications for biomass burning. Chemical Geology 152, 151–161.

Bohlmann, J., Phillips, M., Ramachandiran, V., Katoh, S., Croteau, R., 1999. cDNA cloning, characterization, and functional expression of four new monoterpene synthase members of *Tpsd* gene family from grand fir (*Abies grandis*). Archives of Biochemistry and Biophysics 368, 232–242.

Chang, S.-T., Chen, P.-F., Wang, S.-Y., Wu, H.-H., 2001. Antimite activity of essential oils and their constituents from *Tiwania cryptomerioides*. Journal of Medical Entomology 38, 455–457.

Chikaraishi, Y., Naraoka, H., 2003. Compound-specific δD-$\delta^{13}C$ analysis of *n*-alkanes extracted from terrestrial and aquatic plants. Phytochemistry 63, 361–371.

Collister, J.W., Rieley, G., Stern, B., Eglinton, G., Fry, B., 1994. Compound-specific $\delta^{13}C$ analyses of leaf lipids from plants with differing carbon dioxide metabolisms. Organic Geochemistry 21, 619–627.

Cvejic, J.H., Rohmer, M., 2000. CO_2 as main carbon source for isoprenoid biosynthesis via the mevalonate-independent methylerythritol 4-phosphate route in the marine diatoms *Phaeodactylum tricornutum* and *Nitzschia ovalis*. Phytochemistry 53, 21–28.

Deines, P., 1980. The isotope composition of reduced organic carbon. In: Fritz, P., Fontes, J.Ch. (Eds.), Handbook of Environmental Isotope Geochemistry, The Terrestrial Environment A. Elsevier, Amsterdam Oxford New York, pp. 329–406.

DeNiro, M.J., Epstein, S., 1977. Mechanism of carbon isotope fractionation associated with lipid synthesis. Science 197, 177–185.

DeNiro, M.J., 1981. The effects of different methods of preparing cellulose nitrate on the determination of the D/H ratios of non-exchangeable hydrogen of cellulose. Earth and Planetary Science Letters 54, 177–185.

Eglinton, G., Hamilton, R.J., 1967. Leaf epicuticular waxes. Science 156, 1322–1335.

Eisenreich, W., Rohdich, F., Bacher, A., 2001. Deoxyxylulose phosphate pathway to terpenoids. Trends in Plant Science 6, 78–84.

Epstein, S., Yapp, C.J., Hall, J.H., 1976. The determination of D/H ratios of non-exchangeable hydrogen in cellulose extracted from aquatic and land plants. Earth and Planetary Science Letters 30, 241–251.

Killops, S.D., Killops, V.J., 1993. Chemical composition of biogenic matter. In: Gill, R.C.O. (Ed.), An Introduction to Organic Geocehmistry. John Wiley, Sons, Inc, New York, pp. 22–62.

Kleining, H., 1989. The role of plastids in isoprenoid biosynthesis. Annual Reviews of Plant Physiology and Plant Molecular Biology 40, 39–59.

Kolattukudy, P.E., 1976. Chemistry and Biochemistry of Natural Waxes. Elsevier, Amsterdam.

Hayes, J.M., Freeman, K.H., Popp, B.N., Hoham, C.H., 1989. Compound-specific isotopic analyses: a novel tool reconstruction for ancient biogeochemical processes. Organic Geochemistry 16, 1115–1128.

Hayes, J.M., 1993. Factors controlling ^{13}C contents of sedimentary organic compounds: principles and evidence. Marine Geology 113, 111–125.

Hayes, J.M., 2001. Fractionation of carbon and hydrogen isotopes in biosynthetic processes. In: Valley, J.W., Cole, D.R. (Eds.), Reviews in Mineralogy and Geochemistry 43, Stable Isotope Geochemistry. The Mineralogical Society of America, Washington, pp. 225–277.

Hilkert, A.W., Douthitt, C.B., Schlüter, H.J., Brand, W.A., 1999. Isotope ratio monitoring gas chromatography/mass spectrometry of D/H by high temperature conversion isotope ratio mass spectrometry. Rapid Communications in Mass Spectrometry 13, 1226–1230.

Lange, B.M., Rujan, T., Martin, W., Croteau, R., 2000. Isoprenoid biosynthesis: the evolution of two ancient and distinct pathways across genomes. PNAS 97, 13172–13177.

Lichtenthaler, H.K., Rohmer, M., Schwender, J., 1997. Two independent biochemical pathways for isopentenyl diphosphate and isoprenoid biosynthesis in higher plants. Physiologia plantarum 101, 643–652.

Lichtenthaler, H.K., 1999. The 1-deoxy-D-xylulose-5-phosphate pathway of isoprenoid biosynthesis in plant. Annual Reviews of Plant Physiology and Plant Molecular Biology 50, 47–65.

Lockheart, M.J., van Bergen, P.F., Evershed, R.P., 1997. Variations in the stable carbon isotope compositions of individual lipids from the leaves of modern angiosperms: implications for the study of higher land plant-derived sedimentary organic matter. Organic Geochemistry 26, 137–153.

Lockheart, M.J., Poole, P.F., van Bergen, P.F., Evershed, R.P., 1998. Leaf cabon isotope compositions and stomatal character: important considerations for palaeoclimate reconstructions. Organic Geochemistry 29, 1003–1008.

Luo, Y.-H., Sternberg, L., Suda, S., Kumazawa, S., Mitsui, A., 1991. Extremely low D/H ratios of photoproduced hydrogen by cyanobacteria. Plant Cell Physiology 32, 897–900.

Monson, K.D., Hayes, J.M., 1982. Carbon isotope fractionation in biosynthesis of bacterial fatty acids. Ozonolysis of unsaturated fatty acids as a means of determining the intramolecular distribution of carbon isotopes. Geochimica et Cosmochimica Acta 46, 139–149.

Reddy, C.M., Eglinton, T.I., Palic, R., Benitez-Nelson, B.C., Stojanovic, G., Palic, I., Djordjevic, S., Eglinton, G., 2000. Even carbon number predominance of plant wax *n*-alkanes: a correction. Organic Geochemistry 31, 331–336.

Rieley, G., 1994. Derivatization of organic compounds prior to gas chromatographic-combustion-isotope ratio mass spectrometric analysis: identification of isotope fractionation processes. Analyst 199, 915–919.

Sessions, A.L., Burgoyne, T.W., Schimmelman, A., 1999. Fractionation of hydrogen isotope in lipid biosynthesis. Organic Geochemistry 30, 1193–1200.

Sessions, A.L., Jahnke, L.L., Schimmelmann, A., Hayes, J.M., 2002. Hydrogen isotope fractionation in lipids of the methane-oxidizing bacterium *Methlococcus capsulatus*. Geochimica et Cosmochimica Acta 66, 3955–3969.

Smith, B.N., Esptein, S., 1970. Biogeochemistry of the stable isotopes of hydrogen and carbon in salt marsh biota. Plant Physiology 46, 738–742.

Yakir, D., DeNiro, M.J., 1990. Oxygen and hydrogen isotope fractionation during cellulose metabolism in *Lemna gibba L.* Plant Physiology 93, 325–332.